



ORIGINAL ARTICLE

A Comprehensive Study of Proton-Proton Elastic Scattering

J.P. Gupta

Department of Physics, D.S. College Aligarh (UP) India

Email: jpgupta9412328924@rediffmail.com

ABSTRACT

The hadron-hadron elastic scattering is of crucial importance in understanding the process of hadron-nucleus interactions. The analysis of p - p differential elastic scattering cross-section ($d\sigma/dt$), the ratio of the elastic scattering cross-section to the total cross-section (σ_{el}/σ_{tot}) at ISR energies and Tevatron energies, during last five decade or so, have opened new era in high energy physics. In the present work, an effort is made to present a review to understand the mechanism of p - p elastic scattering. The differential elastic scattering cross-section for a wide range of energy have been studied, in which a considerable minima (Dip) is observed. The studies of the position of the dip (t_{dip}), the position of the secondary maxima (t_{max}), the differential elastic scattering cross-section at the dip ($(d\sigma/dt)_{dip}$) and at the second maxima ($(d\sigma/dt)_{second\ max}$) and their energy dependence are taken into account.

Key words: p - p interaction, p -scattering, scattering cross-section, h - h scattering

Received: 4th May 2017, Revised: 25th May 2017, Accepted: 27th May 2017

©2017 Council of Research & Sustainable Development, India

How to cite this article:

Gupta J.P. (2017): A Comprehensive Study of Proton-Proton Elastic Scattering. Annals of Natural Sciences, Vol. 3[2]: June, 2017: 137-144.

INTRODUCTION

The measurements and analysis of proton-proton (p - p) and proton-antiproton (p - \bar{p}) total cross-sections, differential elastic scattering cross-sections, the ratio of real to imaginary parts of nuclear amplitudes and the total slope parameter, at high energies have opened a new era in high energy physics, during last five decay or so (Amos *et al.*, 1990 and the ref. there in And Block *et al.*, 2016 and the ref. there in). The total cross-section (σ_{tot}) is one of the basic parameter of scattering processes in the sum of several cross-sections of all accessible final states.

The fundamental properties of hadrons (π^+ , π^- , π^0 , p , \bar{p} , etc) e. g, the wave nature of colliding hadrons, the finite range of their strong interactions together with their absorptive character etc, are reflected from the differential scattering of hadrons. The main features of proton-proton elastic scattering, is the appearance of a sharp dip (minima) at four momentum transfer square $t \approx 1.4$ (GeV/c)², in the differential elastic scattering cross-section, when it varies with t (Fig. 1&2), followed by a secondary maxima. Several authors and scientists (Abazov, *et al.*, 2012 And Castaldi 1985 and the ref. there in) have made comprehensive studies of dip structure and its energy dependence. The dip becomes more and more pronounced as the energy increases and then it recedes. The position of the dip moves inward on increasing the energy (Negy, *et al.*, 1979).

At high energies, proton-proton elastic scattering is believed to be well described by a single scalar (Amaldi *et al.*, 1973), mainly imaginary amplitude and it is usually assumed that as energy increases, the role of spin becomes negligible and the interaction becomes mostly absorptive, dominated by many open inelastic channels. Elastic scattering is then essentially the shadow of the inelastic cross-section. Therefore, the elastic amplitude has a diffractive character in close analogy with the diffraction of plane wave in classical optics.

PRESENT WORK

In the present article, a brief review on proton-proton elastic scattering process is presented and an effort is made to understand the mechanism of differential scattering of p-p interactions. The differential elastic scattering cross-section for a wide range of energy has been studied, in which a considerable minima (Dip) is observed. The studies of the position of the dip (t_{dip}), the position of the secondary maxima (t_{max}), the differential elastic scattering cross-section at the dip $(d\sigma/dt)_{dip}$ and at the second maxima $(d\sigma/dt)_{second\ max}$ and their energy dependence are taken into account.

PROTON-PROTON ELASTIC SCATTERING

The differential elastic scattering cross-section may be expressed as the sum of three terms,

$$d\sigma/dt = \sigma_C + \sigma_I + \sigma_N \quad \dots\dots (1)$$

where σ_C , σ_I and σ_N are the Coulomb, interference and nuclear contributions respectively. In a very forward direction ($t < 10^{-3} \text{GeV}^2$), the elastic differential cross-section is dominated by the real coulomb amplitude (Castaldi 1985). The magnitude of Coulomb and nuclear amplitudes are of the same order, for the value of 't' between 10^{-3} and 10^{-2}GeV^2 and may give rise to a non-negligible interference effect (Amaldi *et al.*, 1977). The most striking feature of high energy proton-proton elastic scattering is the division of the angular distribution of the scattering cross-section into three distinct regions of momentum transfer (Fig. 2) (Alsad *et al.*, 1983). The regions may be characterized, qualitatively as following-

1. In the $0.001 \leq |t| \leq 0.01 \text{ GeV}^2$ region, the Coulomb nuclear interference effect becomes more and more important as the incident energy increases.
2. For $0.01 \leq |t| \leq 1.0 \text{ GeV}^2$, there is a sharp forward peak (Fig. 1). This part of the angular distribution is weakly energy dependent (Breakstone *et al.*, 1984). The forward peak is generally, recognized to be diffractive or shadow scattering phenomenon caused by the absorptive processes in high energy p-p collisions. As a result, the forward scattering amplitude is mainly imaginary.
3. For $|t| > 1.0 \text{ GeV}^2$, the angular distributions are much flatter than described in (ii) and have very strong energy dependence (Alsad *et al.*, 1983).

THE REGION OF COULOMB - NUCLEAR INTERFERENCE

Several authors (Negy *et al.*, 1979 and Block *et al.*, 2016 and the ref. there in) fitted the p-p and p- \bar{p} differential cross-section using the parameterization,

$$d\sigma/dt = \pi [f_c + f_n]^2 \quad \dots\dots (2)$$

where the Coulomb amplitude,

$$f_c = \pm 2\alpha [G^2(t)/|t|] \cdot \exp(\mp i\alpha\Phi) \quad \dots\dots (3)$$

And the nuclear scattering amplitude,

$$f_n = [(1+\rho)/4\pi] \cdot \sigma_{tot} \exp(-b|t|/2) \quad \dots\dots (4)$$

In the above expression (3), $G(t) = [1 + |t| / (0.71)]^{-2}$ is the proton electro-magnetic form factor, α is the fine structure constant and $(\alpha\Phi)$ is the Coulomb phase factor. In Eqn. (3) the upper sign is for $p-\bar{p}$ and the lower sign is for $p-p$ scattering. The total cross-section σ_{tot} is introduced through the optical theorem, ' ρ ' is the ratio of the real to imaginary part of f_n and ' b ' is the slope parameter.

The relative importance of the interference term (Eqn.2) is minimum when the nuclear and Coulomb amplitudes are comparable (at $-t \approx 8\pi\alpha / \sigma_{tot}$). The contribution of the interference term to the cross-section in a first approximation is $\approx [-(\pm)(\rho+\Phi)\alpha\sigma_{tot}] / |t|$, and can easily be distinguished from the steeper $1/t^2$ dependence of the Coulomb term and from the relatively flat nuclear contribution (Fig.3) (Castaldi *et al.*, 1985). If the factor $(\rho+\Phi)$ is positive, the interference is destructive for $p-p$ and constructive for $p-\bar{p}$ scattering and the interference has the reverse behaviour when $(\rho+\Phi)$ is negative.

The measurement of the interference term allows the determination of the phase of the nuclear scattering amplitude ' F ' in the forward direction, which is usually expressed as the ratio (ρ) of the real to imaginary part of the scattering amplitude at the four momentum transfer $t = 0$, i.e,

$$(\rho) = [\text{Re } F(s,t) / \text{Im } F(s,t)] \quad \text{..... (5)}$$

The real part of the elastic amplitude is related to the imaginary part via dispersion relation (Bronzan *et al.*, 1974). On the other hand the imaginary part at $t = 0$, it is related to the total cross-section by the Optical theorem. As a consequence, it is possible to write the parameter (ρ) at a given energy as an integral of the total cross-section over energy. Such an integral relation can be approximated by a local expression, which relates (ρ) to the derivative of σ_{tot} with respect to energy.

$$(\rho) = (\pi / 2 \sigma_{tot}) \quad d\sigma_{tot}/d \ln s \quad \text{..... (6)}$$

THE DIFFRACTION PEAK REGION ($|t| \leq 1 \text{ GeV}^2$)

The data on $p-p$ elastic scattering along with corresponding $p-\bar{p}$ data are shown in Fig. 1. In this figure Break-stone *et al.* reported the results of the measurement $p-p$ and $p-\bar{p}$ elastic scattering at c.m. energies $\sqrt{s} = 31, 53$ and 62 GeV . The data is represented by an exponential dependence on the four momentum transfer t i.e,

$$d\sigma/dt = a \exp(bt) \quad \text{..... (7)}$$

Where, ' a ' and ' b ' are two adjustable parameters.

The energy dependence of the slope of elastic differential cross-section for $p-p$ and $p-\bar{p}$ scattering indicates shrinkage of the diffraction peak at a rate of at least $\ln s$ (Burg *et al.*, 1982). In the simplest Optical model, the description of diffraction scattering, the parameter ' b ' measured at $|t| \rightarrow 0$, is proportional to the square of the proton radius. The essential energy dependence or shrinking of the diffraction peak is characterized by the increase of ' b ' with energy.

The energy dependence of the slope of the elastic differential cross-sections for $p-p$ and $p-\bar{p}$ scattering (Fig.1) appears, to behave exactly the same way on increasing the energy (Burg *et al.*, 1982). Such behaviour is expected at asymptotic energies, since the Cornille-Martine theorem, $[(d\sigma/dt)\bar{a} b] / [(d\sigma/dt)ab] \rightarrow 0$, states that the elastic differential cross-sections of the particle-particle and particle-antiparticle, in the region of the diffraction peak tends to be the same for $s \rightarrow \infty$.

THE LARGE t -REGION

The main feature of the $p-p$ elastic differential cross-section in t -region is a progressive development, up to ISR energies (Castaldi *et al.*, 1985), of a sharp dip around $t \sim 1.4 \text{ GeV}^2$, as shown in Fig. 2.

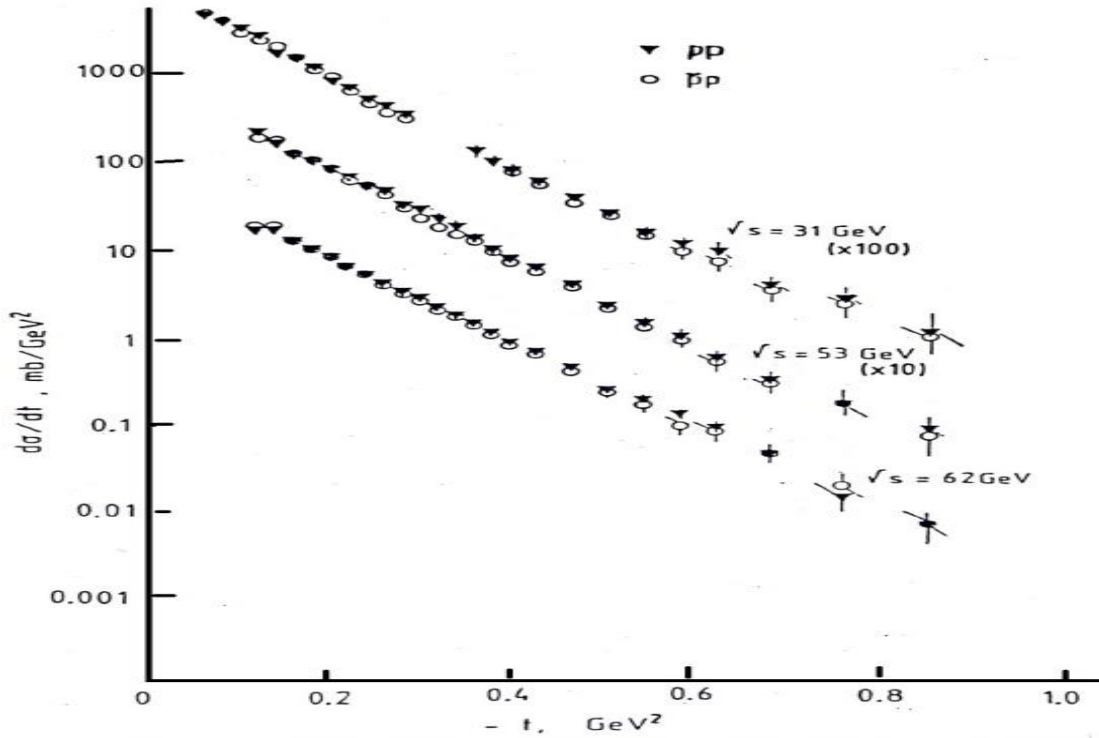


Fig. 1: Diffraction Peaks at ISR Energies in Proton-Proton & Proton-Antiproton Elastic Scattering

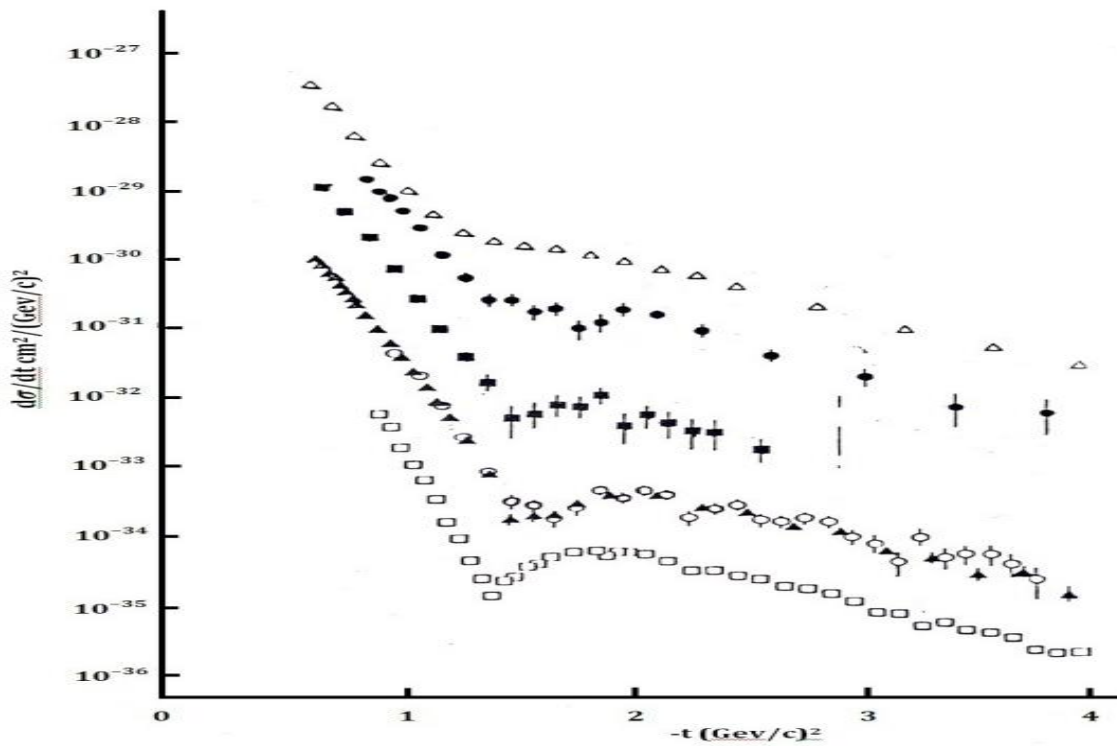


Fig. 2: Progressive Development of the DIP-Bump Structure in Proton-Proton Elastic Differential Cross-Section

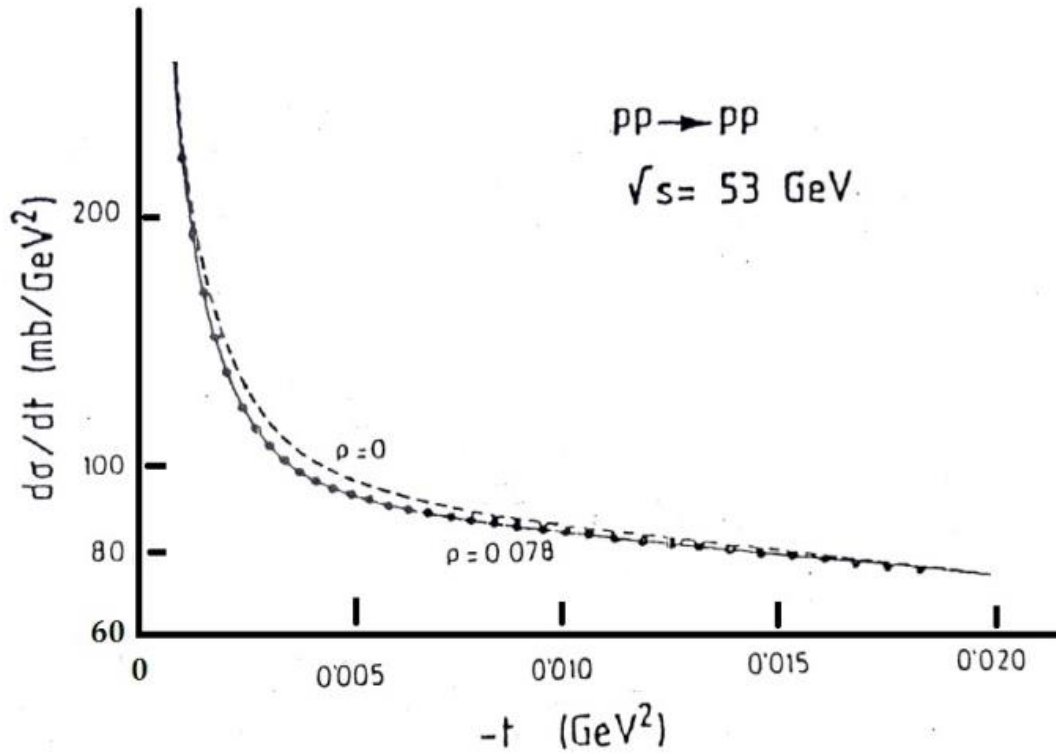


Fig. 3: Differential Cross-Section for Proton-Proton Elastic Scattering in the Coulomb Region

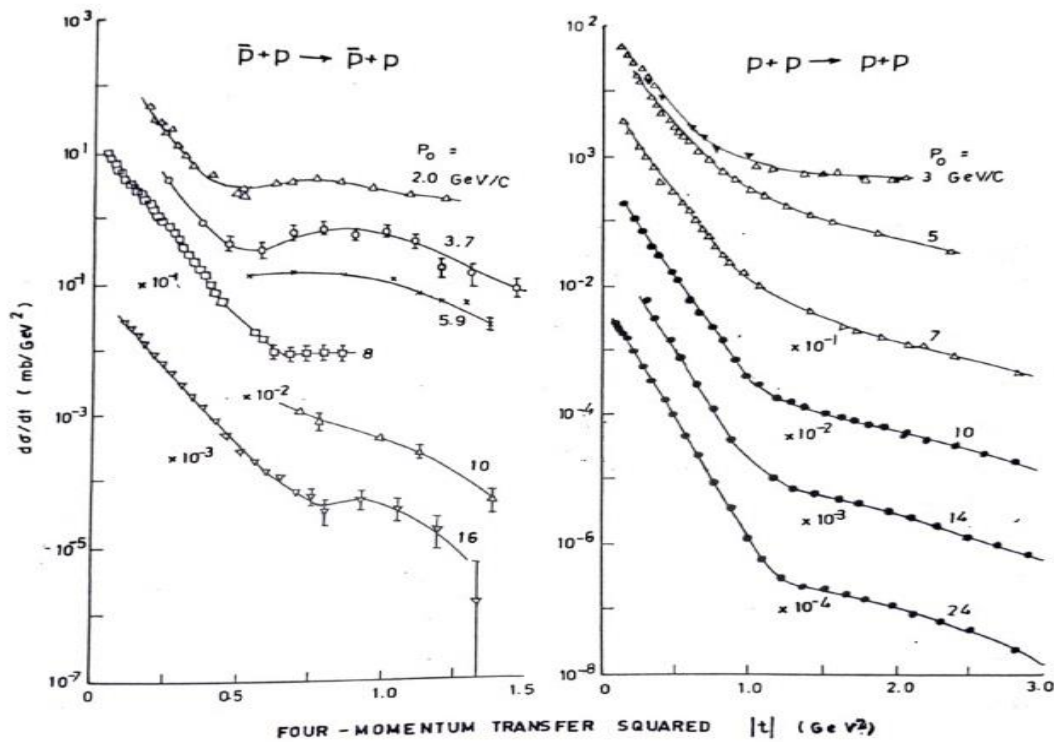


Fig. 4: Comparison of Angular Distributions of Proton-Proton & Proton-Antiproton Elastic Scattering

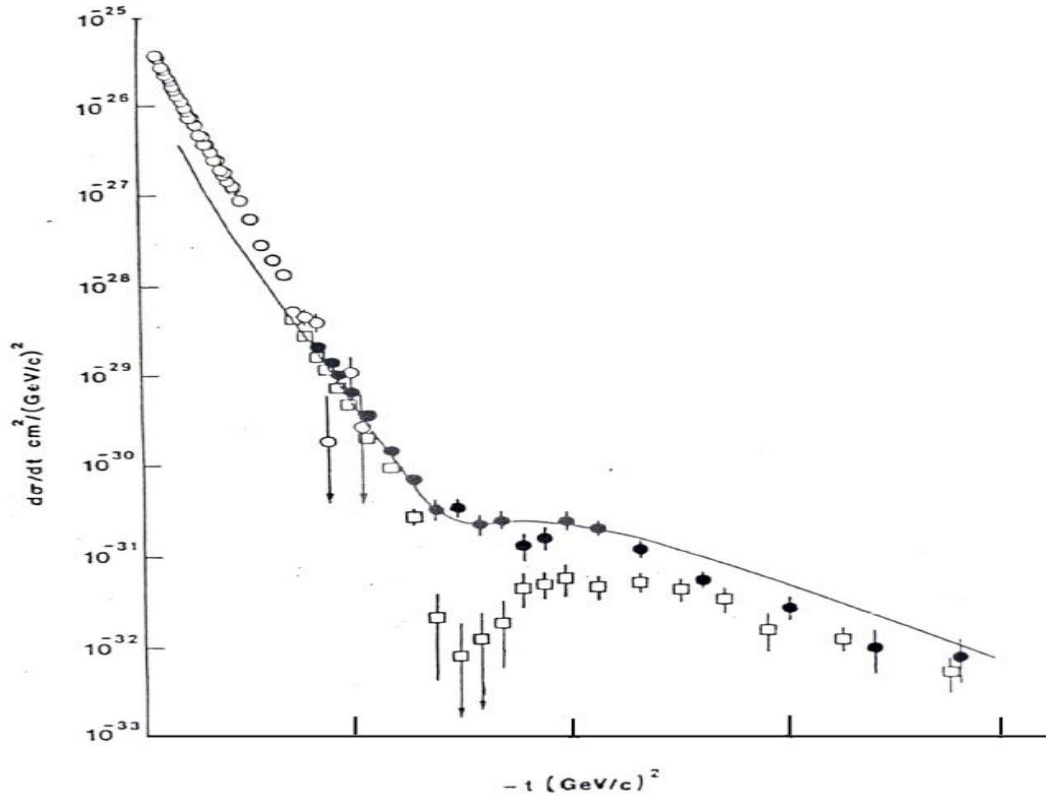


Fig. 5: Comparison of Dip-Bump Structure in p-p and P- \bar{p} Elastic Scattering at 50 GeV/c

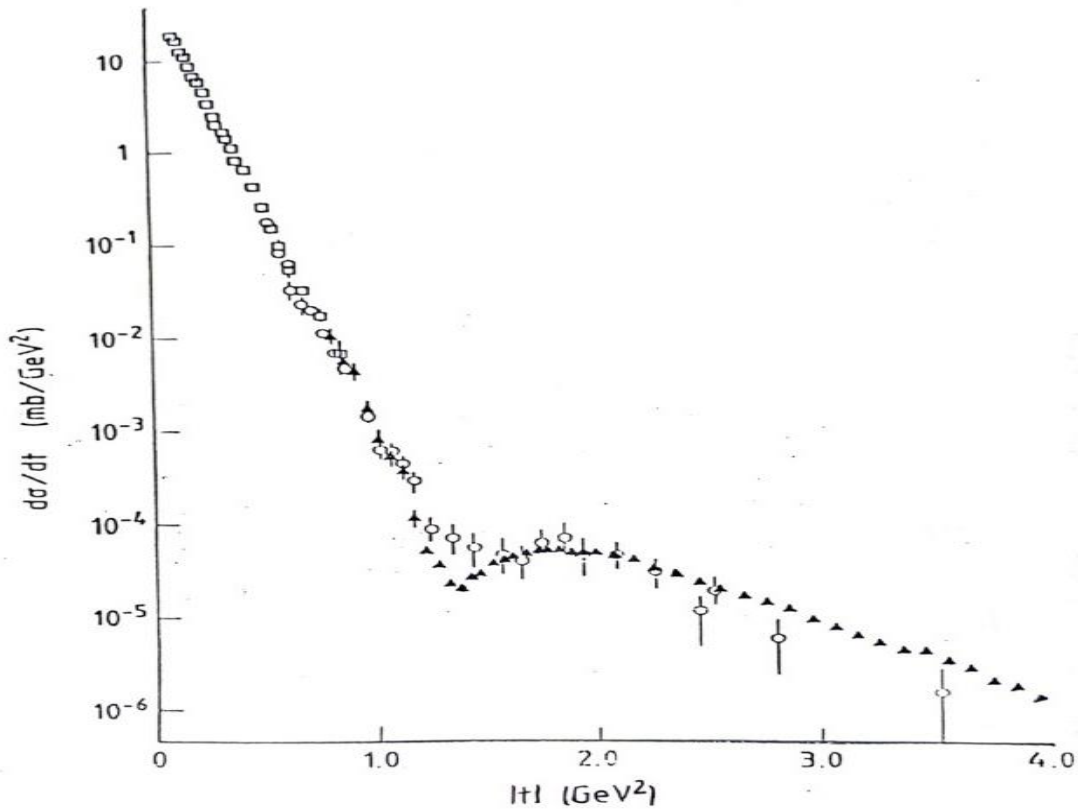


Fig. 6: Comparison of Dip-Bump Structure in p-p and P- \bar{p} Elastic Scattering at 1500 GeV/c

The position of the dip is observed to move toward smaller $|t|$ values, while the height of the secondary maxima grows in the ISR energy range. At much lower energies, no dip is observed in the differential cross-section distribution for proton-proton scattering, but only a break of slope can be observed (alsad *et al.*, 1983), at $|t| \approx 1.5 \text{ GeV}^2$. It is only above, $p_{lab} \sim 50 \text{ GeV}/c$, that a diffraction like dip structure becomes clearly visible. On the other hand the differential cross-section distribution for proton-antiproton elastic scattering shows a sharp dip even at very low beam momentum, 30 GeV/c and 50 GeV/c (Fig. 4). The position of the dip in proton-antiproton elastic scattering at these low energies moves outwards, while at ISR energies, it was found to move inwards with increasing total cross-section (Castaldi *et al.*, 1985).

The $p\text{-}\bar{p}$ distribution at $|t| \sim 1.4 \text{ GeV}^2$ indicates possible different behaviour w.r.t. the $p\text{-}p$ distribution and seems to exhibit shoulder rather than a clear dip, at $p_{lab} \sim 50 \text{ GeV}/c$ (Fig. 5). The differences in $p\text{-}p$ and $p\text{-}\bar{p}$ differential cross-sections (Fig.6) appear to diminish as the incident energy increases and it is reasonable to assume that the Cornille-Martine prediction is essentially verified beyond ISR (Castaldi *et al.*, 1985).

CONCLUSIONS

1. The differential scattering cross-section, as a function of four momentum transfer (t), shows a diffraction character. The position of the dip shifts inward on increasing the incident energy.
2. The differential scattering cross-section at the dip, depends not only on the behavior of $(\rho\sigma_{tot})^2$, but it depends also on the t -dependent behaviour of $(d\sigma/dt)$ in the peak region.
3. The $(d\sigma/dt)$ at second maxima and also on the deviation of its position from the position of the second maxima maximum height.
4. Some authors explained the dip and the diffractive peak on the basis of Quantum Chromo Dynamics (QCD), according to which, three gluon exchange give rise to a crossing odd component in the diffractive peak that can account for a shoulder in $p\text{-}\bar{p}$ and for a dip in $p\text{-}p$ at the same time.
5. A large amount of theoretical and phenomenological work has been done to understand the complex features $p\text{-}p$ and $p\text{-}\bar{p}$ differential cross-sections. Some important models are, (i) s -channel Model (ii) Eikonal Model (iii) Shadow Scattering Model (iv) Geometrical Scaling (v) Constituent Model (vi) Single scattering Model (vii) Multi Scattering Model etc.

REFERENCE

1. Abazov, V.M. *et al.*, (2012): Observation of a narrow mass state decaying in $p\text{-}\bar{p}$ collisions at 1.96 TeV. Phys. Rev. D 86: 12009.
2. Alsad, Z. *et al.*, (1983): Proton-proton elastic scattering at 50 GeV/c incident momentum, Phys. Lett. B 128: 124.
3. Amaldi, U. *et al.*, (1973): Energy dependence of pp total cross-section for c.m. energies 23-25 GeV. , Phys. Lett. B 44: 112.
4. Amaldi, U. *et al.*, (1977): Real part of the forward pp scattering amplitude, Phys. Lett. B 66: 390.
5. Amos, N.A. *et al.*, (1990): A Luminosity independent measurement of pp total cross-section, Phys. Lett. B 243: 158.
6. Avila, C. *et al.*, (2002): The ratio of the real to imaginary part of $p\text{-}\bar{p}$ forward elastic scattering amplitude, Phys. Lett. B 537: 41.
7. Breakstone, A. *et al.*, (1984): A measurement of pp and $p\text{-}\bar{p}$ elastic scattering at ISR energies, Nucl. Phys. B 248: 253.
8. Bronzan, J.B. *et al.*, (1974): Obtaining real parts of scattering amplitudes directly from cross-section data, Phys. Lett. B 49: 272.
9. Burg, J.P. *et al.*, (1982): Experimental results on pp forward elastic scattering, Phys. Lett. B 109: 124.

10. Castaldi, R. *et al.*, (1985): Elastic scattering and total cross-sections at very high energies, *Ann. Rev. Nucl. Part. Sci.* 35: 351.
11. Giacomelli G. and M. Jacob, (1979): Physics at CERN-ISR, *Phys. Rep.* 55: 1.
12. Kaspar, J. *et al.*, (2011): Phenomenological models of elastic nucleon scattering and predictions for LHC, *Nucl. Phys. B* 843: 84.
13. M.M. *et al.*, (2016): Slope, curvature and higher parameters in pp and p- \bar{p} scattering, *Phys. Rev. D* 93: 114009.
14. Negy, E. *et al.*, (1979): Measurement of elastic scattering at large momentum transfer, *Nucl. Phys. B* 150: 221.